Int. J. Heat Mass Transfer. Vol. 36, No. 15, pp. 3663–3669, 1993
Printed in Great Britain

0017–9310/93 $6.00+0.00

Non-Darcy natural convection around a horizontal cylinder buried near the surface of a fluid-saturated porous medium

D. M. CHRISTOPHER and B.-X. WANG
Thermal Engineering Department, Tsinghua University, Beijing 100084, China

(*Received* 18 *February* 1993 *and in final form* 7 *April* 1993)

Abstract—Natural convection around a horizontal, isothermal cylinder buried in a fluid-saturated porous medium is modeled analytically using the Forchheimer-extended Darcy flow model. The governing equations are solved numerically to obtain the flow field, the temperature distribution, and the local and average Nusselt numbers around the cylinder as functions of the cylinder depth, H, the modified Rayleigh number, Ra^*, and the Darcy number, Da. The results show that the presence of an impermeable surface above the cylinder significantly alters the flow field and reduces the heat transfer from the cylinder. Recirculating zones may develop above the cylinder creating regions of low and high heat transfer rates. The Forchheimer term in the velocity equation reduces the flow velocity and, hence, the heat transfer for the case of large Darcy number and results in a significant decrease in the average Nusselt number around the cylinder when Re_d is greater than approximately five.

INTRODUCTION

NUMEROUS works in the literature analyzed the natural convection in a fluid-saturated porous medium along vertical plates or constrained in rectangular enclosures but few papers reported results for natural convection around a horizontal cylinder in a fluid-saturated porous medium. However, the natural convection around a buried oil or steam pipeline or a long set of buried nuclear waste canisters surrounded by water-saturated soil needs to be modeled using the equations for flow in fluid-saturated porous media. Our current work considers a pipeline or canister buried in water-saturated soil relatively near the soil surface or near an impermeable cover layer. The proximity of this surface drastically alters the flow field in the porous medium and reduces the heat transfer. The geometry is idealized as an infinite, isothermal, horizontal cylinder buried in a fluid-saturated porous medium with an impermeable surface above the cylinder. The flow field around the cylinder and the convective heat transfer away from the cylinder are modeled analytically. Previous work [1] has suggested that even if the surface is 50 or more diameters away from the pipe, the flow field and heat transfer will still be affected.

The heat transfer and flow field around a buried pipeline were previously analyzed by Bau [2] for small modified Rayleigh numbers and small Darcy numbers. He obtained a series solution to the governing equations based on the Darcy flow model and then developed a Nusselt number correlation for Darcy flow and small values of the modified Rayleigh number as functions of the modified Rayleigh number and the cylinder depth. Fand *et al.* [3] reported similarity solutions using Darcy's model for natural convection heat transfer from a horizontal cylinder embedded in an infinite porous medium. Recently, Nakayama and Pop [4] proposed an unified similarity transformation for free, forced and mixed convection in an infinite medium using both the Darcy model and the Forchheimer-extended Darcy flow model.

In this paper, the Forchheimer-extended Darcy model for flow in a fluid-saturated porous medium is used to describe the flow in the porous medium. The flow is assumed to be incompressible and two-dimensional (r, θ). The porous medium is assumed to be uniform, isotropic, and in local thermodynamic equilibrium with the saturating fluid. Steady-state solutions are obtained. However, the numerical solution procedure uses the transient energy equation to facilitate convergence. Steady-state flow fields and Nusselt number distributions are presented for various values of the governing parameters: the modified Rayleigh number, Ra^*, the Darcy number, Da, and the cylinder depth, H.

MATHEMATICAL MODEL

Steady-state free convection flow around a cylinder buried in a fluid-saturated porous medium (Fig. 1) is modeled with the Forchheimer-extended Darcy model for flow in porous media. Using dimensionless variables and incorporating Boussinesq's approximation, the governing equations relating the pressure drop and the flow rate, in polar coordinates (r, θ), are:

$$-\frac{\partial P}{\partial r}-\left[1+\frac{c\sqrt{Da}}{Pr}|V|\right]u-Ra^*\sin(\theta)T=0 \quad (1)$$

$$-\frac{1}{r}\frac{\partial P}{\partial \theta}-\left[1+\frac{c\sqrt{Da}}{Pr}|V|\right]v-Ra^*\cos(\theta)T=0. \quad (2)$$

NOMENCLATURE

- c inertial coefficient in Forchheimer extension
- D cylinder diameter
- Da Darcy number, k/R_1^2
- g gravitational constant
- H distance from cylinder centerline to upper surface
- k permeability
- Nu_{R_1} Nusselt number, equation (9)
- P pressure
- Pr Prandtl number
- Q_{cond} conduction heat transfer from the cylinder
- r radial coordinate
- R computational domain outer radius
- R_1 cylinder radius
- Ra^* modified Rayleigh number, $kg\beta(t-t_\infty)R_1/\nu\alpha$
- Re_d particle Reynolds number
- t temperature
- T dimensionless temperature excess
- u radial velocity
- v angular velocity
- x horizontal coordinate
- y vertical coordinate.

Greek symbols

- α thermal diffusivity
- β thermal expansion coefficient
- θ angular coordinate (horizontal = 0)
- λ thermal conductivity
- ν kinematic viscosity
- τ Fourier number, $\alpha t/R_1^2$
- ψ stream function.

The velocity magnitude is defined as: $|V| = (u^2+v^2)^{1/2}$. The angle θ in Fig. 1 is taken to be zero at the horizontal axis. The value of the inertia coefficient in the Forchheimer extension, c, was found to have a nearly constant value of about 0.55 [5].

The continuity equation is:

$$\frac{1}{r}\frac{\partial(ru)}{\partial r}+\frac{1}{r}\frac{\partial v}{\partial \theta}=0. \tag{3}$$

The velocity equations along with the continuity equation can be combined to give the following scalar pressure equation in dimensionless form:

$$\frac{1}{r}\frac{\partial}{\partial r}\left(Ar\frac{\partial P}{\partial r}\right)+\frac{1}{r^2}\frac{\partial}{\partial \theta}\left(A\frac{\partial P}{\partial \theta}\right) = Ra^*\left[-\frac{\sin(\theta)}{r}\frac{\partial}{\partial r}(AT)-\frac{1}{r}\frac{\partial}{\partial \theta}(A\cos(\theta)T)\right] \tag{4}$$

where the coefficient

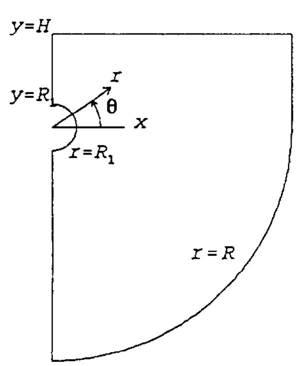

FIG. 1. Geometry.

$$A=\left[1+\frac{c\sqrt{Da}}{Pr}|V|\right]^{-1}.$$

The non-dimensionalized energy equation is:

$$\frac{\partial T}{\partial \tau}+u\frac{\partial T}{\partial r}+\frac{v}{r}\frac{\partial T}{\partial \theta}=\frac{1}{r}\frac{\partial}{\partial r}\left(r\frac{\partial T}{\partial r}\right)+\frac{1}{r^2}\frac{\partial^2 T}{\partial \theta^2} \tag{5}$$

where T is the dimensionless temperature excess,

$$T(r,\theta) = [t(r,\theta)-t(r=R)]/[t(R_1,\theta)-t(r=R)].$$

The boundary conditions are symmetric about the centerline:

$$T(R_1,\theta)=1 \qquad T(R,\theta)=0$$

$$T(x,y=H)=0 \qquad \frac{\partial T}{\partial \theta}\left(r,\pm\frac{\pi}{2}\right)=0 \tag{6a}$$

outflow/inflow boundary condition: $P(R,\theta) = 0$. (6b)

The surfaces at $y = H$, $r = R_1$, and $\theta = \pm\pi/2$ are impermeable. R_1 is the cylinder radius and R is a radius large enough to act as the outer radius of the computational domain. Since both outflow and inflow at the outer computational boundary, $r = R$, are convection dominated, the temperature boundary condition at $r = R$ in equation (6a), is equivalent to setting the temperature equal to zero at infinity [1] and results in a simpler computational scheme. This boundary condition will be discussed further with the numerical results. The outflow/inflow pressure boundary condition at $r = R$ in equation (6b), is a consequence of assuming that the angular velocity, v, equals zero at the sufficiently large outer radius of the computational domain. The temperature is also essentially zero so that, from equation (2), $\partial P/\partial\theta = 0$.

Therefore, the pressure along the entire outer computational radius is equal to a constant which is selected to be zero. The pressure boundary condition at the outer boundary allows the flow to leave the upper part of the outer boundary, recirculate outside of the computational domain and reenter along the lower region of the outer boundary. The resulting extended flow field has been shown [1] to be a more realistic representation of the flow because the boundary does not artificially restrict the flow to a limited domain.

For H/R_1 less than 40, an outer computational radius, R, equal to $50R_1$ was found to be adequate to reasonably represent the heat transfer and the flow field near the cylinder without requiring an excessively large computational domain. For H/R_1 equal to 40, the outer computational radius was increased to $65R_1$ to obtain a reasonable grid arrangement.

Inspection of equations (4)–(6) shows that the governing parameters are the modified Rayleigh number, Ra^*, the cylinder depth, H, and the parameter $c\,Da^{1/2}/Pr$. Since we desire to study the effect that various Darcy numbers have on the flow and heat transfer, the Prandtl number in the third governing parameter was held constant for a given fluid in the saturated porous media. Therefore, the third governing parameter is simply the Darcy number.

The local Nusselt number is defined relative to purely conductive heat transfer from the pipe per unit length:

$$Nu = \frac{-2\pi\lambda R_1 \left.\dfrac{\partial T}{\partial r}\right|_{R_1}}{Q_{\mathrm{cond}}}. \tag{7}$$

Bau [2] has shown that the conduction heat transfer per unit length of pipe is:

$$Q_{\mathrm{cond}} = \frac{2\pi\lambda R_1}{\cosh^{-1}(H)}. \tag{8}$$

Therefore, the Nusselt number is simply:

$$Nu_{R_1} = -\left.\frac{\partial T}{\partial r}\right|_{R_1} \cosh^{-1}(H). \tag{9}$$

NUMERICAL METHOD

Equations (4) and (5) were solved using MARIAH, a finite-element code [6] for analyzing flow in fluid-saturated porous medium. Each solution involved over 3000 non-uniformly spaced nodes and nearly 1000 elements clustered near the cylinder, especially in the region between the cylinder and the upper surface. Figure 2 shows part of the computational grid for $H/R_1 = 10$.

Various grid arrangements were tested to verify the consistency of the results. Using substantially less elements and nodes (over 1500 nodes and approximately 500 elements) resulted in a less than 4% change in the average Nusselt number along the cylinder.

The grid parameter having the greatest influence over the accuracy of the results was the thickness of the first radial element. The thickness of the first radial element had to be less than $0.01R_1$ to obtain consistent and accurate results for various geometries. Different grid arrangements were used for different cylinder depths to appropriately model the different flow fields. These different grid arrangements all concentrated grid points near the cylinder and in the region above the cylinder and were designed so that the thickness of the first radial element was always less than $0.01R_1$. While efforts were made to obtain accurate results, the grid arrangements used for the calculations were, of course, a trade-off between accuracy and computer time.

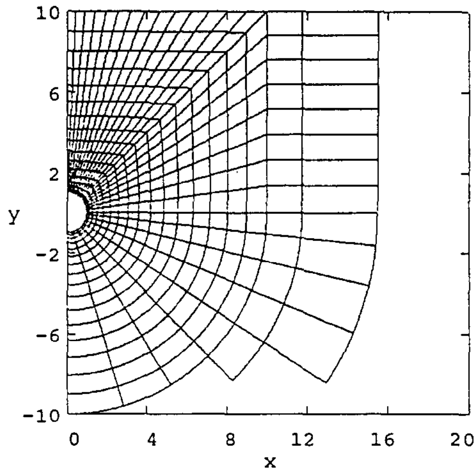

FIG. 2. Computational grid for $H/R_1 = 10$.

Calculations were performed on 386 or 486 personal computers. For the greatest number of nodes, the computing time was more than 15 h.

RESULTS WITH DISCUSSION

Equations (4) and (5) with the boundary conditions specified by equation (6) were solved numerically for modified Rayleigh numbers from 1 to 400, Darcy numbers from pure Darcy flow to $Da = 10^{-4}$, and cylinder depths from 2 to 40.

Part of a typical flow field for pure Darcy flow with $H/R_1 = 4$ and $Ra^* = 10$ is shown in Fig. 3. The flow field is visualized using the standard definition of the stream function in cylindrical coordinates. The flow rises due to buoyancy from below the cylinder. Heat conducted horizontally away from the cylinder also causes fluid far from the cylinder to rise due to buoyancy. Because of the horizontal impermeable surface at $H/R_1 = 4$, the fluid turns away from the vertical centerline, a line of symmetry. Some of the fluid is seen to recirculate within the computational domain while the rest of the fluid recirculates far from the cylinder.

The temperature distribution for pure Darcy flow

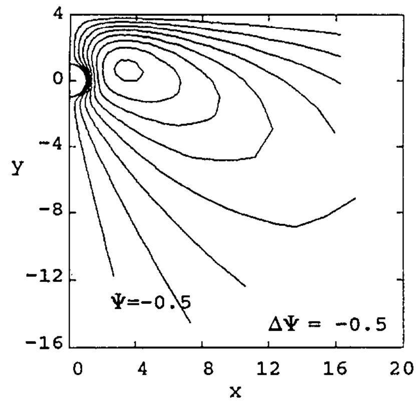

FIG. 3. Streamlines for $Ra^* = 10$ and $H/R_1 = 4$.

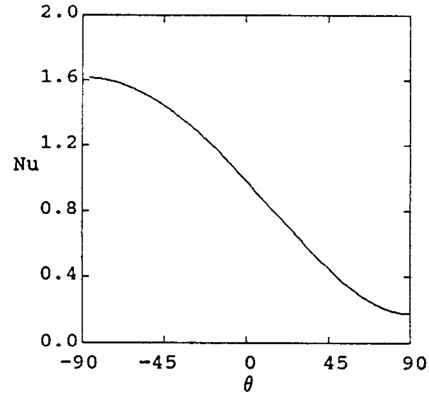

FIG. 5. Local Nusselt numbers for $Ra^* = 10$ and $H/R_1 = 4$.

with $H/R_1 = 4$ and $Ra^* = 10$ is shown in Fig. 4. Below the cylinder outside a radius of approximately 10 R_1, the temperature is essentially equal to the temperature far from the cylinder because the convection heat transfer toward the cylinder is significantly greater than the diffusion against the flow away from the cylinder. Setting the dimensionless temperature excess, T, to zero at the outer boundary of the computational domain, equation (6a), therefore, has no effect on the results. The plume of warm fluid rising above the cylinder is carried to the side as the flow is turned away from the centerline by the upper surface of the domain. The thermal energy in the flow is quickly dissipated by diffusion and by mixing with cooler fluid further away from the cylinder. The fluid temperature is lowered to the ambient temperature long before reaching the outer edge of the computational domain.

The local Nusselt number distribution for pure Darcy flow along the cylinder with $Ra^* = 10$ and $H/R_1 = 4$ is given in Fig. 5. The local Nusselt number is very large on the lower part of the cylinder, since the fluid is flowing towards the surface and the fluid temperature approaching the cylinder is essentially the far field temperature. The local Nusselt number decreases along the cylinder as the boundary layer grows. Near the top where the fluid flows away from the surface, the boundary layer is much thicker and, hence, the Nusselt number is much lower.

For sufficiently large modified Rayleigh numbers (i.e. relatively large fluid velocities) and small cylinder depths, H, a recirculating region develops above the cylinder that substantially alters the heat transfer along the cylinder. As an example, the flow field for $Ra^* = 100$ and $H/R_1 = 2$ is shown in Fig. 6. The main part of the flow circulates in a clockwise direction as in Fig. 3. However, in the region above the cylinder, a second vortex appears rotating in the counter-clockwise direction. As shown by the Nusselt number distribution in Fig. 7, there is a substantial decrease in the heat transfer where the fluid flows away from the surface. The heat transfer is again higher at the top of the cylinder where the fluid flows down toward the cylinder.

For small modified Rayleigh numbers and small cylinder depths, the fluid directly above the cylinder is essentially stagnant, as shown in Fig. 8 for $Ra^* = 10$ and $H/R_1 = 2$. It is well known that the stability cri-

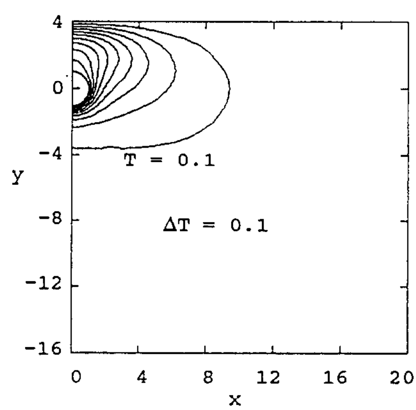

FIG. 4. Isotherms for $Ra^* = 10$ and $H/R_1 = 4$.

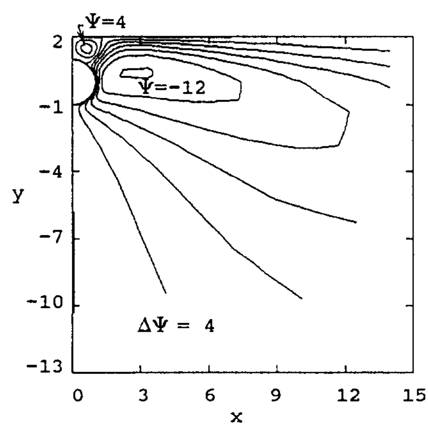

FIG. 6. Streamlines for $Ra^* = 100$ and $H/R_1 = 2$.

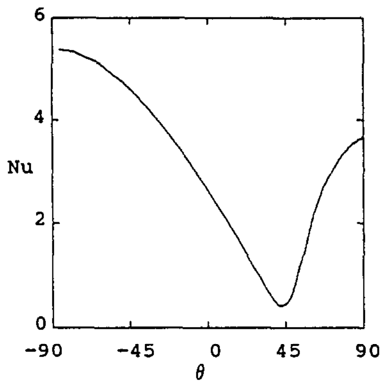

FIG. 7. Local Nusselt numbers for $Ra^* = 100$ and $H/R_1 = 2$.

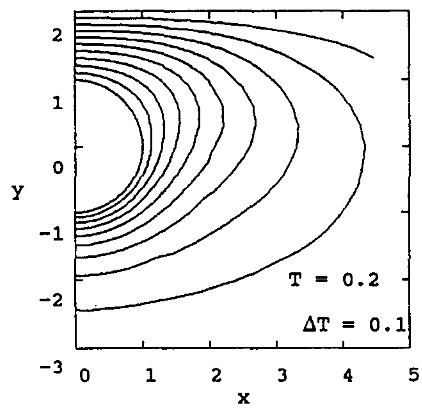

FIG. 9. Isotherms for $Ra^* = 10$ and $H/R_1 = 2$.

terion for the inception of flow in a fluid-saturated porous medium between parallel, isothermal plates is $4\pi^2$. This criterion also serves as a guideline for the presence of significant convection currents in the region above the cylinder in the present geometry. In this region above the cylinder, if the modified Rayleigh number based on the cylinder to top surface spacing (which in this case is equal to the modified Rayleigh number based on the cylinder radius since $H - R_1 = R_1$) is somewhat less than the parallel-plate stability criterion (less than approximately 30), then little convection occurs in the region above the cylinder. As the main flow comes up and around from below the cylinder, it turns outward and begins to recirculate as in Fig. 6. However, since the convective velocities are not great, there is insufficient interaction with the fluid above the cylinder to cause more than a small amount of movement above the cylinder. As a consequence, the heat transfer above the cylinder is mainly due to conduction. The temperature distribution for this situation is shown in Fig. 9 for $Ra^* = 10$ and $H/R_1 = 2$. The uniform spacing of the isotherms above the cylinder indicates that, near the top of the cylinder, the heat transfer from the cylinder to the top surface is mainly by conduction.

For small modified Rayleigh numbers, the average Nusselt numbers along the cylinder are compared with the results of Bau [2] in Fig. 10. Using a series solution, Bau developed an expression for the Nusselt number as a function of the modified Rayleigh number and the cylinder depth for small modified Rayleigh numbers. As can be seen, the present results agree well with Bau's results, especially at low Ra^*. Since Bau's results were derived using a truncated series solution, agreement at larger values of the modified Rayleigh number is not expected.

Average Nusselt numbers along the cylinder are given in Figs. 11, 13, and 14 as functions of the modified Rayleigh number, the cylinder depth, and the Darcy number. For relatively large Rayleigh numbers, $Ra^* = 100$ or greater, the flow field did not reach a steady state due to vortices appearing along the upper surface. Such vortices have been observed in other geometries [7] where warm fluid is flowing along the underside of a cold surface in a porous medium. While the vortices were not insignificant, the fluctuations in

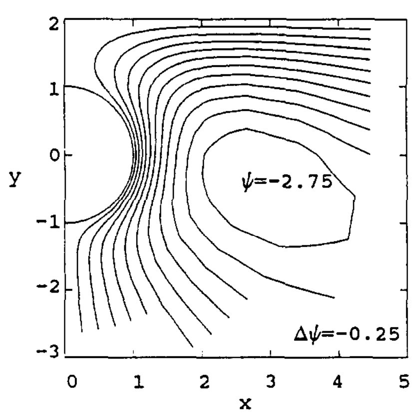

FIG. 8. Streamlines for $Ra^* = 10$ and $H/R_1 = 2$.

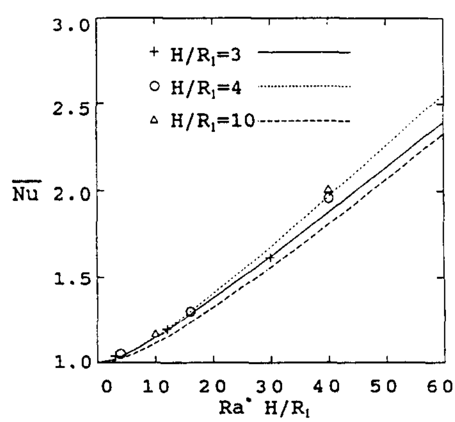

FIG. 10. Comparison of current results (symbols) and results of Bau [2] (lines).

the Nusselt number along the cylinder were less than 1% of the mean values. The Nusselt number values in Figs. 11, 13 and 14 are not only averaged over the cylinder surface but are also averaged in time as well if a steady-state flow field did not develop.

Figure 11 shows results for pure Darcy flow, i.e. when the Forchheimer term is not included in equations (1) and (2) and the coefficient, A, in equation (4) equals 1. The numerical data show that the Nusselt number rapidly increases as the modified Rayleigh number increases due to the increased buoyancy force. The Nusselt number also increases with increasing cylinder depth because the fluid motion is less restricted and the taller buoyancy plumes contribute more to the buoyant force. The relative increase in the buoyant force, however, became less as the depth increased.

As first pointed out by Bau [2] for relatively small modified Rayleigh numbers, an interesting balance occurs between the conduction heat transfer from the cylinder to the top surface; which decreases with increasing cylinder depth; and the convection heat transfer from the top of the cylinder; which increases with increasing cylinder depth. For small modified Rayleigh numbers, the total heat transfer from the cylinder, which is proportional to the average temperature gradient along the cylinder surface (see equation (9)), is minimized at some value of the cylinder depth for a given modified Rayleigh number, Fig. 12. Thus, proper selection of the cylinder depth can reduce the heat loss substantially, more than 50% for $Ra^* = 1$. For modified Rayleigh numbers greater than approximately 20, there is no minimum with increasing depth because the convection is always sufficiently strong to offset the decrease in the conduction heat transfer.

Figure 13 shows results for a large Darcy number, $Da = 10^{-4}$, when the Forchheimer term is significant. The Nusselt number still increases with increasing modified Rayleigh number, but not as rapidly as for pure Darcy flow, Fig. 11. Increasing the cylinder depth

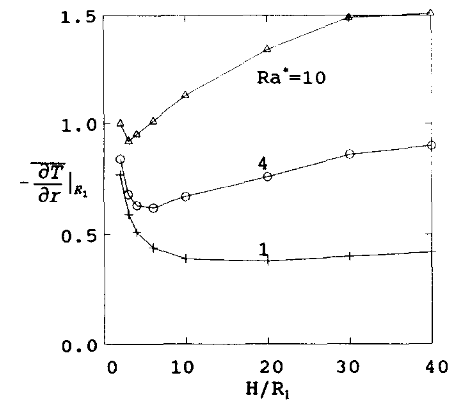

FIG. 12. Heat transfer at small Rayleigh numbers.

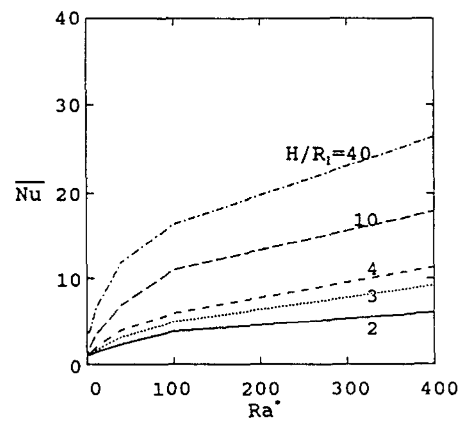

FIG. 13. Nusselt numbers using Forchheimer-extended model, $Da = 10^{-4}$.

also increases the Nusselt number because the fluid motion is less restricted when the cylinder depth is greater.

Figure 14 shows the average Nusselt numbers for

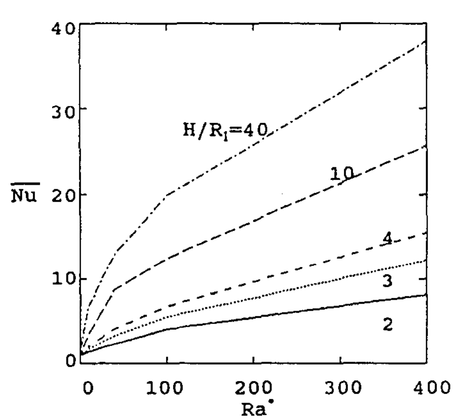

FIG. 11. Average Nusselt numbers using the Darcy flow model.

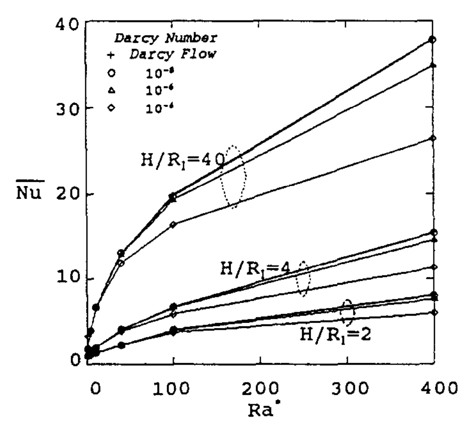

FIG. 14. Average Nusselt numbers for various Darcy numbers and cylinder depths.

several cylinder depths as functions of the modified Rayleigh number and the Darcy number. The results for Darcy number equal to 10^{-8} are essentially the same as pure Darcy flow (no Forchheimer term) so the curves overlap. However, the Nusselt number decreases as the Darcy number is increased to 10^{-6} and 10^{-4}, especially for larger Rayleigh numbers. It is clear from equations (1) and (2) that the addition of the Forchheimer term to the Darcy model results in lower velocities for the same given pressure drop (which is determined by the hydrodynamic pressure far from the cylinder). Although the flow field is altered only slightly by the inclusion of the Forchheimer term, the velocities are sufficiently smaller to cause the Nusselt number to decrease. As seen from equation (4), the Forchheimer term is proportional to the square root of the Darcy number. Therefore, for smaller Darcy numbers, the effect of the Forchheimer term is insignificant. The Forchheimer term is also proportional to the velocity squared. Therefore, it becomes much more significant at higher modified Rayleigh numbers where the velocities are much higher. For $Ra^* = 1$, the differences are insignificant. However, the Nusselt number for larger modified Rayleigh numbers and for larger Darcy numbers is less than for pure Darcy flow because of the significance of the Forchheimer term. Analysis of the numerical results showed that for a maximum Reynolds number based on particle diameter greater than one, inclusion of the Forchheimer term caused a decrease in the average Nusselt number along the cylinder. However, the decrease was not significant until the Reynolds number based on particle diameter was approximately five. This criterion compares well with the standard view that the Darcy model is applicable only when the Reynolds number based on particle diameter is of $O(1)$ or less.

CONCLUSIONS

The heat transfer along a cylinder buried near the surface of a fluid-saturated porous media has been shown to depend strongly on the cylinder depth as well as the modified Rayleigh number. When the cylinder is even as deep as ten cylinder radii below the surface, the heat transfer is significantly reduced because the flow field is restricted by the upper surface. For high modified Rayleigh numbers and when the cylinder is near the surface, a recirculation region develops above the cylinder causing regions of very high and very low heat transfer along the cylinder. For small modified Rayleigh numbers, the balance of conduction and convection heat transfer along the top surface of the cylinder resulted in an optimum burial depth for minimizing the total heat transfer from the cylinder. It was found that the Forchheimer term should be included when the Reynolds number based on particle diameter was approximately five or more.

Acknowledgement—The project was financially supported by the Chinese government's Postdoctoral Research Fund.

REFERENCES

1. D. M. Christopher and B.-X. Wang, Natural convection around a horizontal cylinder in a fluid-saturated porous medium, submitted to *Trans. ASME, J. Heat Transfer* (1992).
2. H. H. Bau, Estimation of heat losses from flows in buried pipes. In *Handbook of Heat and Mass Transfer* (Edited by N. P. Cheremisinoff), Vol. 1, Chap. 32. Gulf Publishing Co., Houston, Texas (1986).
3. R. M. Fand, T. E. Steinberger and P. Cheng, Natural convection heat transfer from a horizontal cylinder embedded in a porous medium, *Int. J. Heat Mass Transfer* **29**, 119–133 (1986).
4. A. Nakayama and I. Pop, A unified similarity transformation for free, forced and mixed convection in Darcy and non-Darcy porous media, *Int. J. Heat Mass Transfer* **34**, 357–367 (1991).
5. J. C. Ward, Turbulent flow in porous media, *ASCE J. Hydraulic Division* **90**, 1–12 (1964).
6. D. K. Gartling and C. E. Hickox, MARIAH—A finite element computer program for incompressible porous flow problems, SAND79-1623, Sandia National Laboratories, Albuquerque, New Mexico (1980).
7. D. M. Christopher, Transient natural convection heat transfer in a cavity filled with a fluid-saturated porous medium, *Proceedings of the Eighth International Heat Transfer Conference, San Francisco, Heat Transfer, 1986*, pp. 2659–2664 (1986).